

# Measurements of the Casimir Force

May 4, 2017

H. B. G. Casimir, On the attraction between two perfectly conducting plates,  
Proceedings of the Royal Netherlands Academy of Arts and Sciences, Vol. 51, pp. 793–795 (1948).

# vacuum energy

Einstein Geometry = Stress-Energy

$$R_{\mu\nu} - \frac{1}{2}Rg_{\mu\nu} + \Lambda g_{\mu\nu} = \frac{8\pi G}{c^4}T_{\mu\nu}$$

Cosmological constant is equivalent to vacuum energy,

$$\Lambda = \frac{8\pi G}{c^2}\rho_{vac}$$

In QFT, each field contributes zero point energy to vacuum energy density,

$$\rho_{vac} \propto (\# \text{polarization states}) \int_0^{k_{cut}} \frac{1}{2}k^3 dk$$

where in principle  $k_{cut} \rightarrow \infty$  but in practice corresponds to energy scale where QFT is expected to be no longer valid.

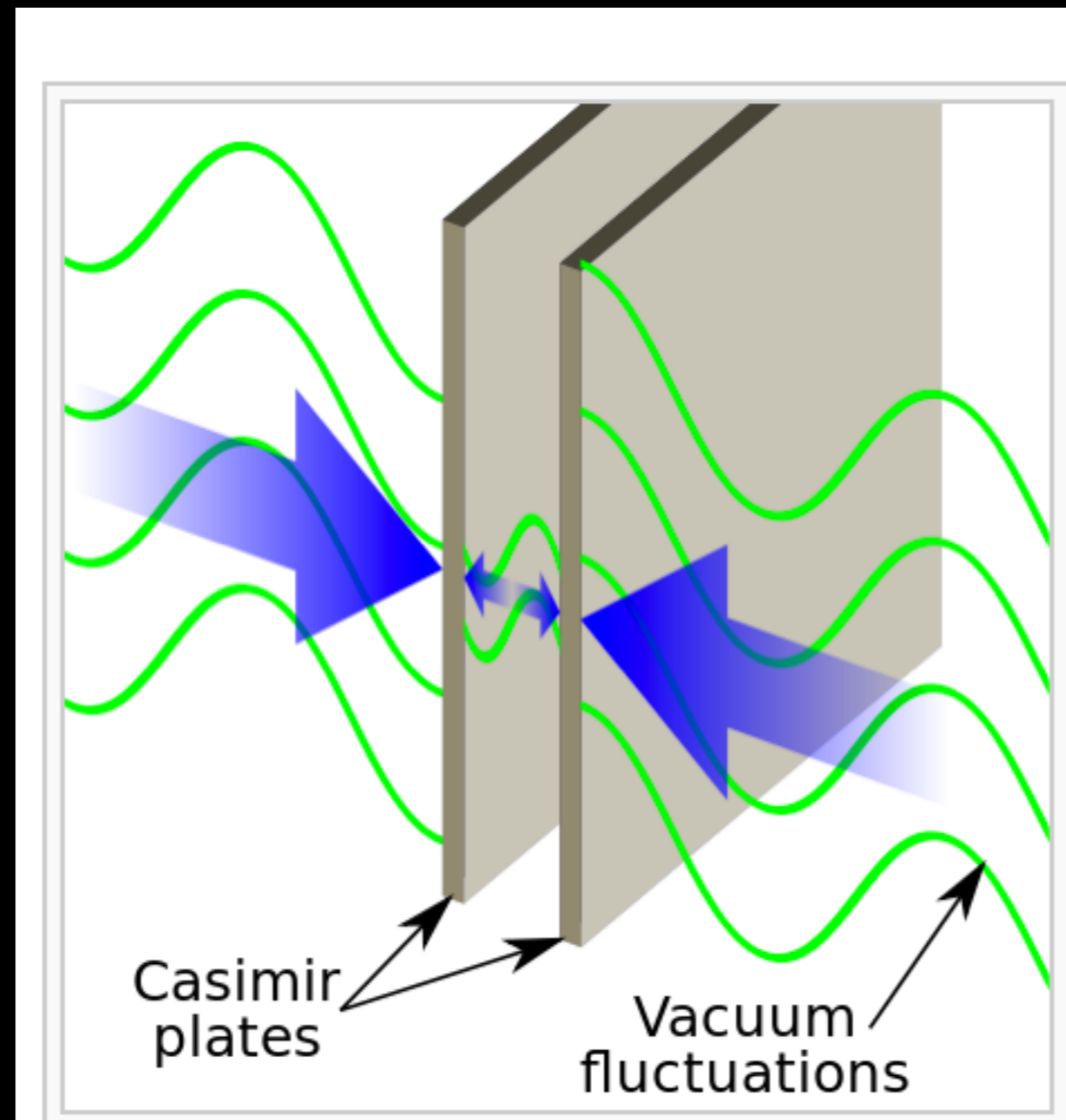
The cosmological constant gives a cosmic repulsive force, for which the observed accelerated expansion of the universe gives evidence for.

Observations give a finite  $\Lambda_{obs}$ , taking  $\hbar k_{cut} = 10^{19}\text{GeV}$  (Planck energy)

$$\Lambda_{theory} = 10^{120}\Lambda_{obs}$$

perfectly conducting plates of area  $A$ , separation  $a$

$$\frac{E - E_0}{A}$$



$$\frac{F}{A} = -\frac{\pi^2 \hbar c}{240 a^4} = -\frac{0.016}{a_{\mu m}^4} \text{dyn/cm}^2$$

minus means attractive

1 dyn = wt of 0.001 g

## Demonstration of the Casimir Force in the 0.6 to 6 $\mu\text{m}$ Range

S. K. Lamoreaux\*

*Physics Department, University of Washington, Box 35160, Seattle, Washington 98195-1560*

*(Received 28 August 1996)*

for sphere of radius  $R$  and flat plate:

between flat plates. Thus, the magnitude of the Casimir force between a sphere and a flat surface is given by

$$F_c(a) = 2\pi R \left( \frac{1}{3} \frac{\pi^2 \hbar c}{240 a^3} \right). \quad (2)$$

and the result is independent of the plate area.

There are at least two corrections to the Casimir force. The first is the effect due to the finite temperature  $T \approx 300$  K; this correction has an illustrious history as discussed by Schwinger *et al.* [9]; the thermal corrections for the Casimir force and van der Waals force are different, and are properly derived for the case of conducting plates in Refs. [9–11]. Taking the results of Brown and Maclay [11], the surface energy is given by  $E = aT^{00}$ , where  $T^{00}$  is the (volume) energy density. Using the PFT and Eq. (20a) of [11], the total magnitude of the Casimir force is

$$F_c^T(a) = F_c(a) \left( 1 + \frac{720}{\pi^2} f(\xi) \right), \quad (3)$$

where  $\xi = kTa/\hbar c = 0.126a \mu\text{m}^{-1}$  at  $T = 300$  K ( $k$  is Boltzmann's constant) and

$$f(\xi) \approx \begin{cases} (\xi^3/2\pi)\zeta(3) - (\xi^4\pi^2/45), & \text{for } \xi \leq 1/2, \\ (\xi/8\pi)\zeta(3) - (\pi^2/720), & \text{for } \xi > 1/2, \end{cases} \quad (4)$$

where  $\zeta(3) = 1.202\dots$ . It is interesting to note that in the large  $a$  limit, the correction is independent of  $\hbar c$  and has the appearance of a classical effect; this is analogous to the Rayleigh-Jeans limit of the black body spectrum.

The second correction, obtained by Schwinger *et al.* [9], is due to the finite conductivity of the plates (modified by the use of the PFT to the case where one plate is spherical);

$$F_c'(a) = F_c(a) \left( 1 + \frac{4c}{a\omega_p} \right), \quad (5)$$

T dependent  
correction

finite conductivity

The Casimir force is closely related to the van der Waals attraction between dielectric bodies. Formally, Eq. (1) is obtained by letting the dielectric constant  $\epsilon$  in the Lifshitz theory [6] approach infinity, which is an appropriate description for a conducting material. However, in practical terms, the Casimir and van der Waals forces are quite different; the van der Waals force is always attractive, whereas the sign of the Casimir force is geometry dependent.

The Casimir force plates comprise a 2.54 cm diam, 0.5 cm thick quartz optical flat, and a spherical lens with radius of curvature 11.3 +/- 0.1 cm and diameter 4 cm; each was coated (by evaporation) with a continuous layer of Cu of thickness 0.5 mm, on all surfaces.



torsion pendulum  
and micro-adjusted  
distance

10<sup>-4</sup> Torr  
eliminates viscosity

Measure change in  
capacitance due to  
separation

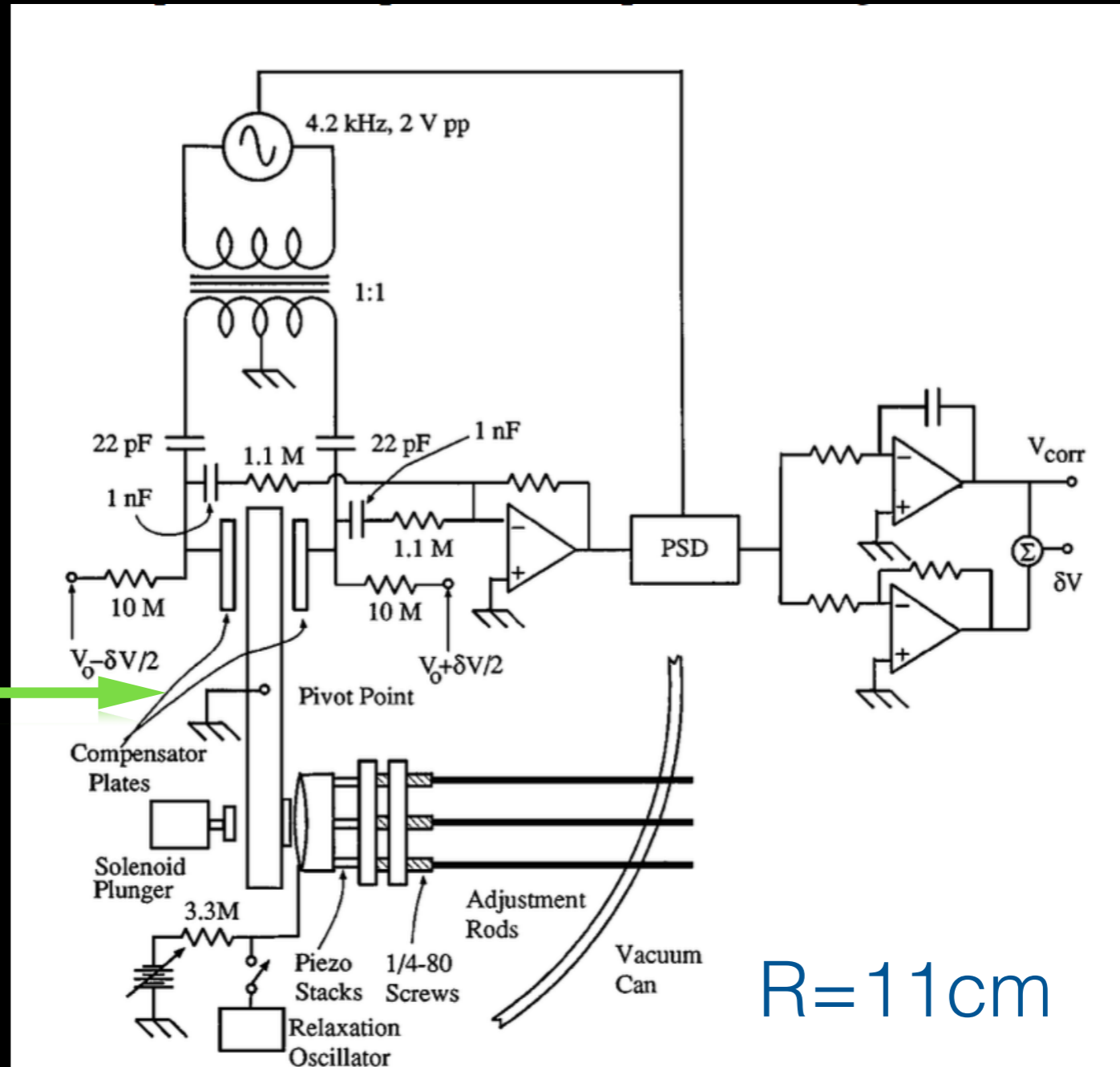


FIG. 1. Schematic of the apparatus. The vacuum vessel dimensions are 55 cm diam by 110 cm tall. The solenoid activated plunger was used to press the plates gently together (during alignment); after such pressing, the plates could be brought much closer.

characteristic

$$|F| \propto a^{-3}$$

Fig. 3. From the absolute position is assigned to  $a_0$  (7), and  $a_i$  is set to  $a_i + a_0$ . Finally, the electrical force is subtracted, giving

$$F_c^m(a_i) = F(a_i) - \frac{\beta}{a_i} - b, \quad (8)$$

where  $F_c^m(a_i)$  is the measured residual force (hopefully the Casimir force). The results of the process, and a direct comparison with the expected Casimir force with no adjustable parameters, is shown in Fig. 3. Typically, the Casimir force had magnitude of at least 20% of the electrical force at the point of closest approach. There was no evidence for a  $1/a^2$  force in any of the data; a force of this form could result from patch effects on the surfaces.

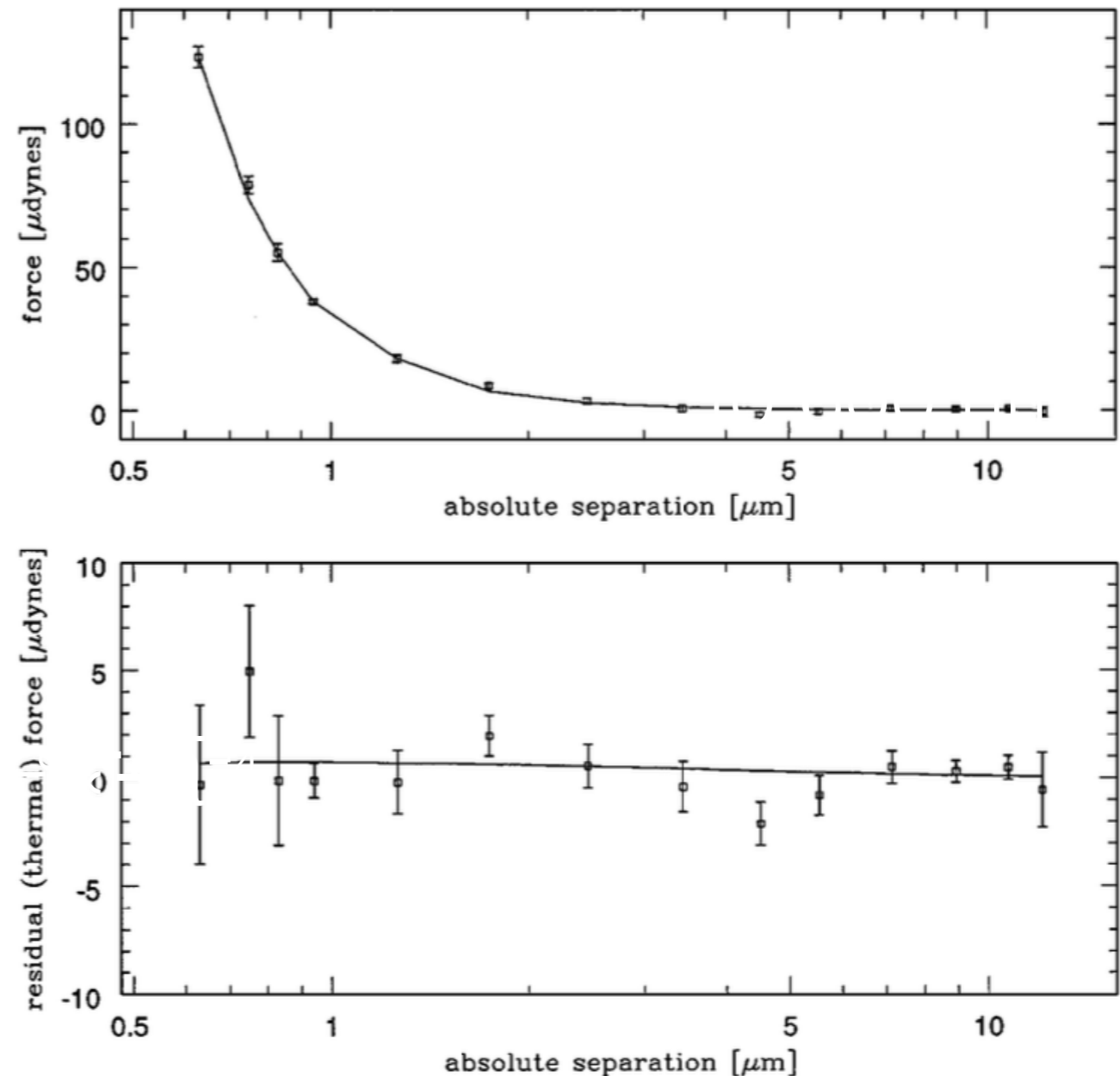


FIG. 4. Top: All data with electric force subtracted, averaged into bins (of varying width), compared to the expected Casimir force for a 11.3 cm spherical plate. Bottom: Theoretical Casimir force, without the thermal correction, subtracted from top plot; the solid line shows the expected residuals.



# **Precision Measurement of the Casimir Force from 0.1 to 0.9 $\mu\text{m}$**

U. Mohideen\* and Anushree Roy

*Department of Physics, University of California, Riverside, California 92521*

(Received 8 May 1998; revised manuscript received 5 October 1998)

As the surfaces are expected to form a boundary to the electromagnetic waves, there is a correction due to the finite conductivity of the metal. This correction to second order based on the free electron model of the reflectivity of metals [13,17] for a given metal plasmon frequency  $\omega_p$  is

$$F_c^p(d) = F_c^0(d) \left[ 1 - 4 \frac{c}{d\omega_p} + \frac{72}{5} \left( \frac{c}{d\omega_p} \right)^2 \right]. \quad (2)$$

Given the small separations  $d$ , there are also corrections to the Casimir force resulting from the roughness of the surface given by [13,14]

$$F_c^R(d) = F_c^p(d) \left[ 1 + 6 \left( \frac{A_r}{d} \right)^2 \right], \quad (3)$$

+ additional term

+ roughness

where  $A_r$  is the average roughness amplitude, and equal roughness for both surfaces has been assumed. There are also corrections due to the finite temperature [12,18] given by

$$F_c(d) = F_c^R(d) \left[ 1 + \frac{720}{\pi^2} f(\xi) \right], \quad (4)$$

where  $f(\xi) = (\xi^3/2\pi)\zeta(3) - (\xi^4\pi^2/45)$ ,  $\xi = 2\pi k_B T d / hc = 0.131 \times 10^{-3} d \text{ nm}^{-1}$  for  $T = 300 \text{ }^\circ\text{K}$ , and  $\zeta(3) = 1.202\dots$ , is the Riemann zeta function, and  $k_B$  is the Boltzmann constant.

same T

deflection measured by laser (diode ratio A/B)

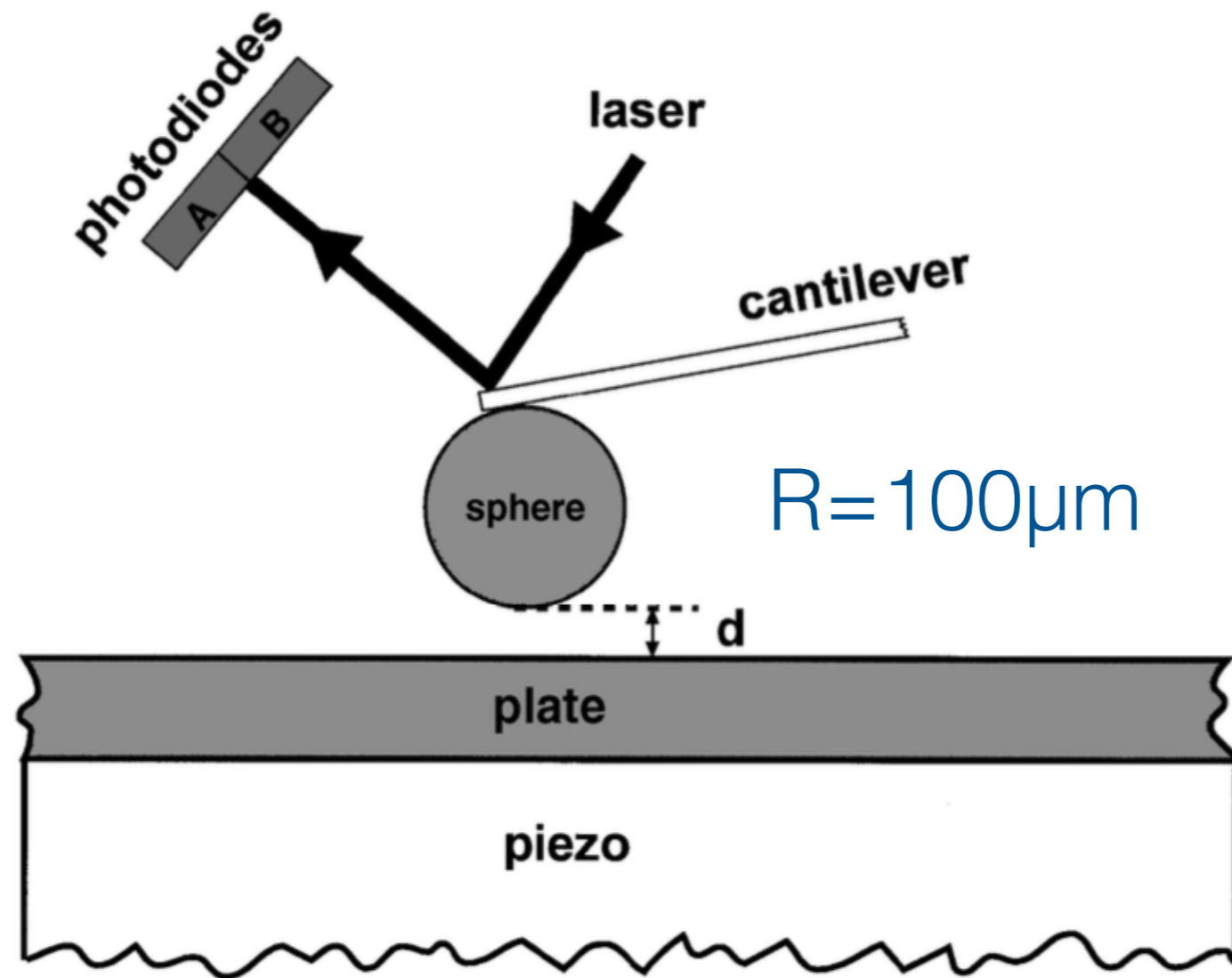


FIG. 1. Schematic diagram of the experimental setup. Application of voltage to the piezo results in the movement of the plate towards the sphere. The experiments were done at a pressure of 50 mTorr and at room temperature.

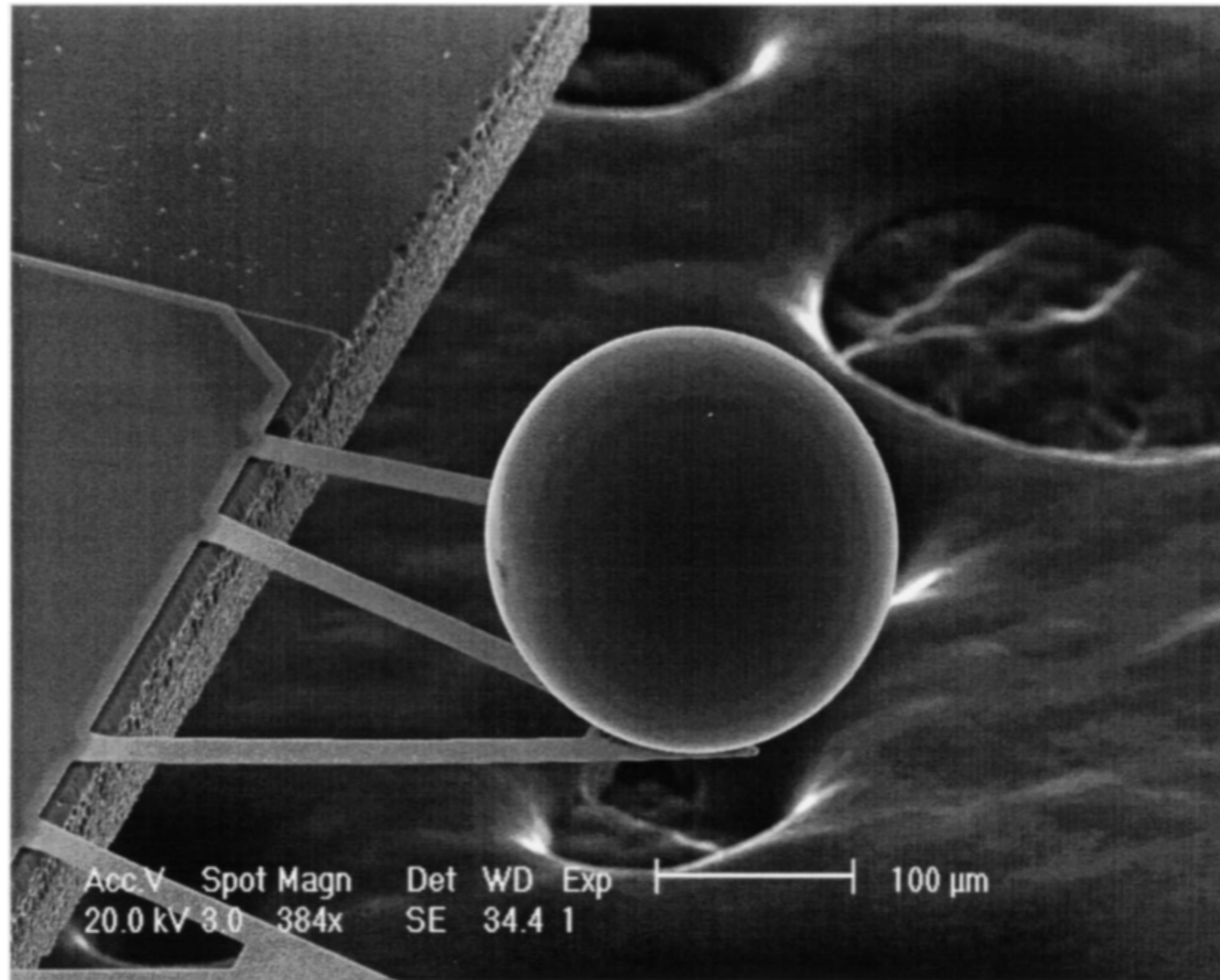


FIG. 2. Scanning electron microscope image of the metallized sphere mounted on a AFM cantilever.



$10^{-12}\text{N} = 10^{-1}\mu\text{dyne}$   
characteristic

$$F \propto -a^{-3}$$

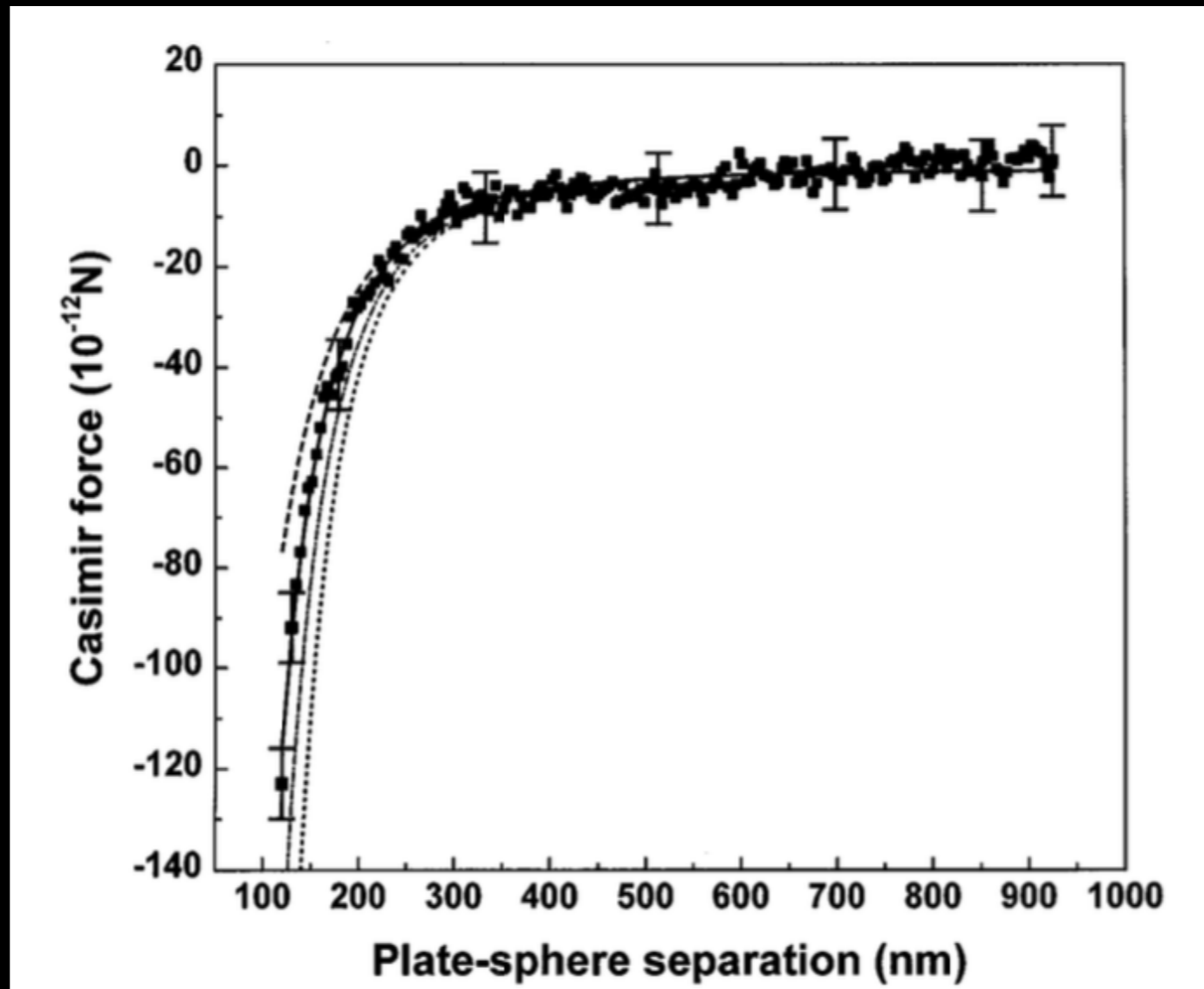


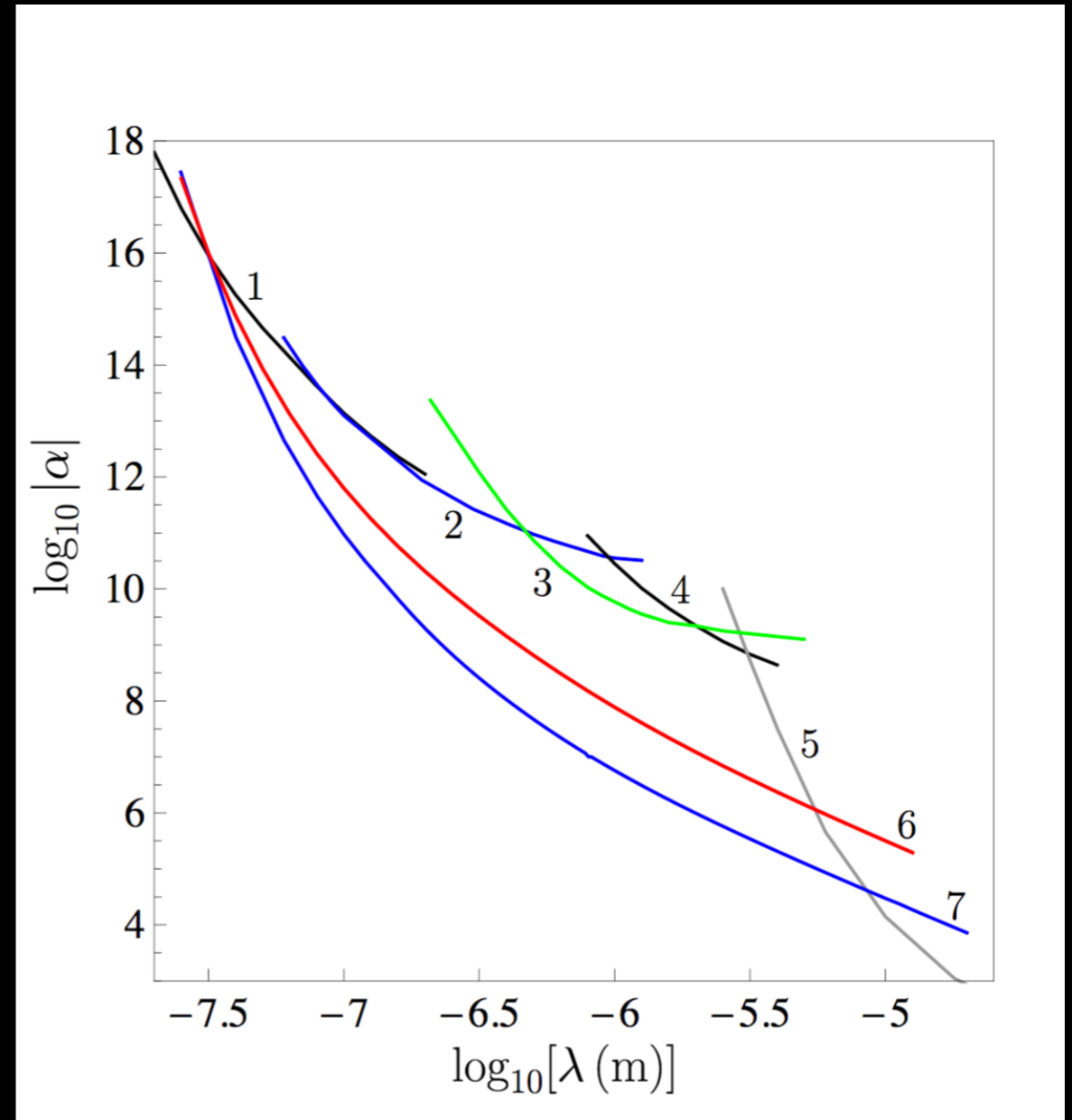
FIG. 4. The measured average Casimir force as a function of plate-sphere separation for 26 scans is shown as square dots. The error bars show the range of experimental data at representative points. The theoretical Casimir force from Eq. (4) with all corrections is shown as a solid line. The rms deviation between the experiment and theory is 1.6 pN. The dash-dotted line is the Casimir force without the finite conductivity, roughness, or temperature correction [Eq. (1)] which results in a rms deviation of 6.3 pN. The dashed line includes only the finite conductivity correction [Eq. (2)] which results in a rms deviation of 5.5 pN. The dotted line includes only the roughness correction leading to a rms deviation of 48 pN.



# Constraints on axion-like particles and non-Newtonian gravity from measuring the difference of Casimir forces

FIG. 3: The line 6 shows the constraints on the strength of Yukawa-type correction to Newton's gravitational law as a function of the interaction length obtained here from the experiment on measuring the difference of Casimir forces. The other lines show previous constraints derived from measuring the effective Casimir pressure (line 1), from previous isoelectronic (Casimir-less) experiment (line 2), from experiment on measuring the difference of lateral forces (line 3), from measuring the Casimir force by means of torsion pendulum (line 4), from the Cavendish-type experiments (line 5), and from the recent isoelectronic experiment (line 7). The regions of the plane above each line are excluded and below each line are allowed.

<https://arxiv.org/pdf/1704.05892.pdf>



# The Casimir effect and the quantum vacuum

*R. L. Jaffe*

Phys.Rev. D72 (2005) 021301

<https://arxiv.org/pdf/hep-th/0503158.pdf>

Despite the simplicity of Casimir's derivation based on zero point energies, it is nevertheless possible to derive his result without any reference to zero point fluctuations or even to the vacuum. Such a derivation was first given by Schwinger for a scalar field, and then generalized to the electromagnetic case by Schwinger, DeRaad, and Milton. Reviewing their derivation, one can see why the zero point fluctuation approach won out. It is far simpler.

I have presented an argument that the experimental confirmation of the Casimir effect does not establish the reality of zero point fluctuations. Casimir forces can be calculated without reference to the vacuum and, like any other dynamical effect in QED, vanish as  $\alpha \rightarrow 0$ . The vacuum-to-vacuum graphs (See Fig. 1) that define the zero point energy do not enter the calculation of the Casimir force, which instead only involves graphs with external lines. So the concept of zero point fluctuations is a heuristic and calculational aid in the description of the Casimir effect, but not a necessity.

# Proof that Casimir force does not originate from vacuum energy

Phys.Lett. B761 (2016) 197-202

<https://arxiv.org/pdf/1605.04143.pdf>

“The true origin of the Casimir force is van der Waals  
force...”

understanding  
correction  
details

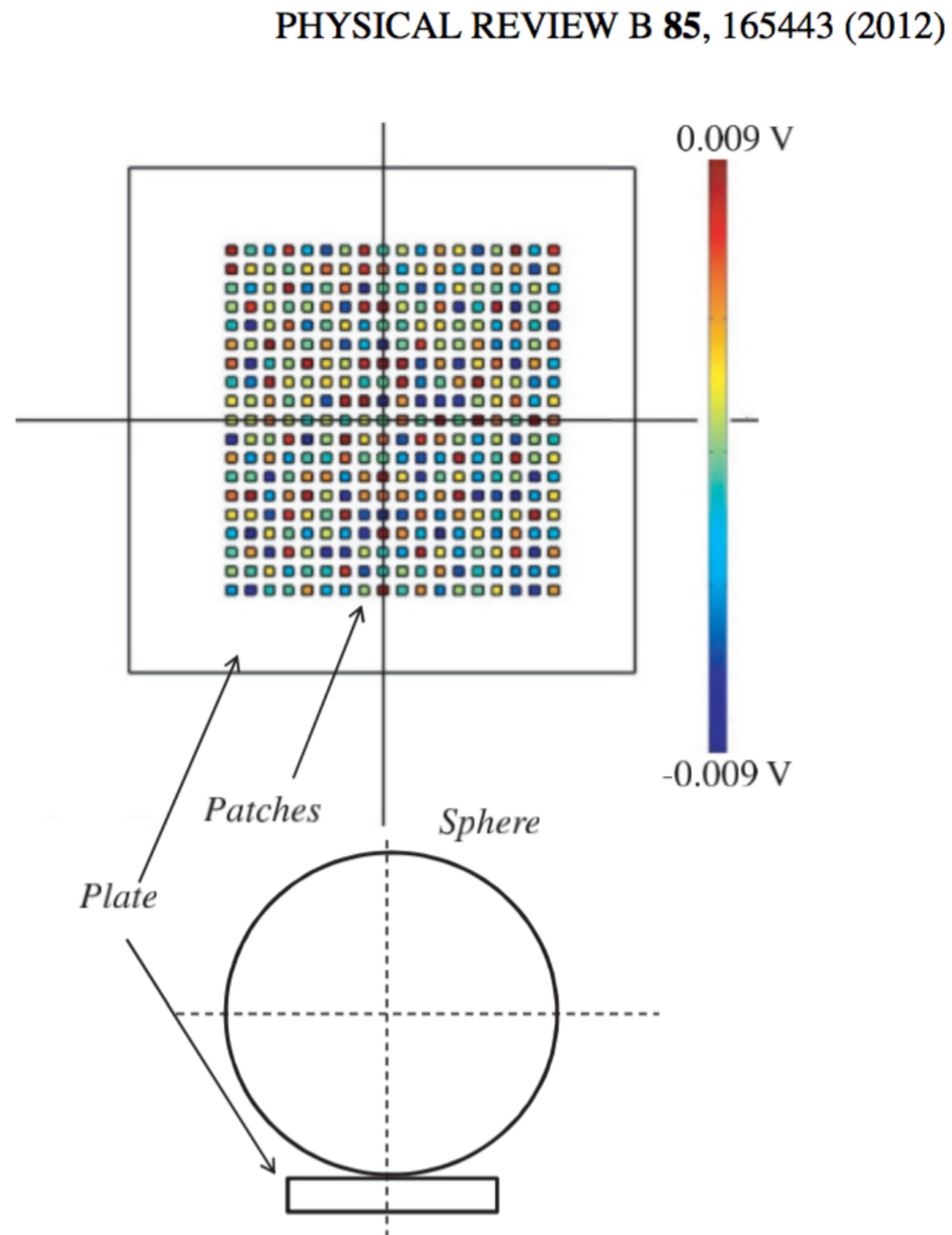


FIG. 2. (Color online) The sphere-plate configuration with patches that were put on the top of a plate.



## Kelvin probe force microscopy of metallic surfaces used in Casimir force measurements

R. O. Behunin,<sup>1</sup> D. A. R. Dalvit,<sup>2</sup> R. S. Decca,<sup>3</sup> C. Genet,<sup>4</sup> I. W. Jung,<sup>5</sup> A. Lambrecht,<sup>6</sup> A. Liscio,<sup>7</sup> D. López,<sup>5</sup>  
S. Reynaud,<sup>6</sup> G. Schnoering,<sup>4</sup> G. Voisin,<sup>3,8</sup> and Y. Zeng<sup>2,\*</sup>

PHYSICAL REVIEW A **90**, 062115 (2014)

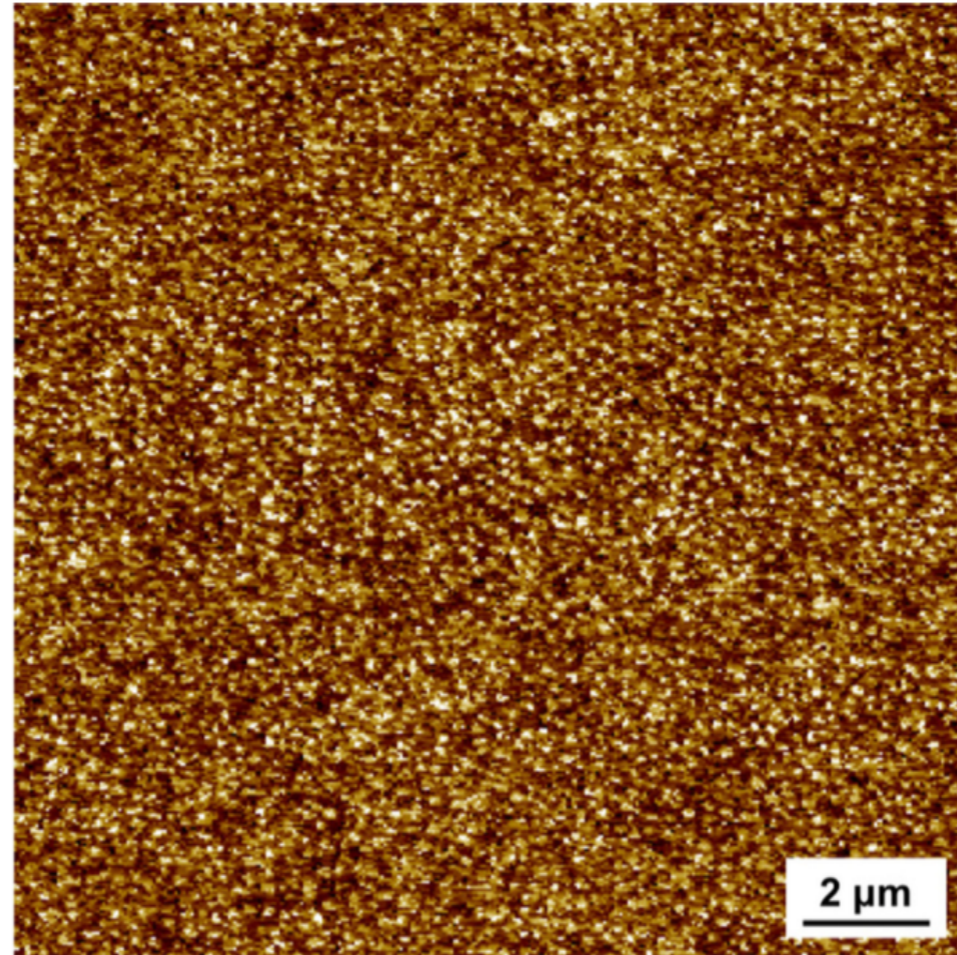


FIG. 2. (Color online) KPFM image of the electrostatic potential distribution  $V_p(\mathbf{x})$  on the surface of the Au sample recorded at ISOF. This image is composed of  $512 \times 512$  pixels, with a lateral size of  $15.36 \mu\text{m}$ . The scale bar corresponds to  $2 \mu\text{m}$  and the scan range is 20 mV. The amplitude of the modulation is  $V_1 = 2.5 \text{ V}$ .

Kelvin probe force  
microscopy